Synthesis, Bioactivity, and Cloning of the L-Type Calcium Channel Blocker ω-Conotoxin TxVII†

Toru Sasaki,‡ Zhong-Ping Feng,§ Randolph Scott,|| Nikita Grigoriev,§ Naweed I. Syed,§ Michael Fainzilber,|| and Kazuki Sato*,‡

Mitsubishi Kasei Institute of Life Sciences, 11 Minamiooya, Machida-shi, Tokyo 194-8511, Japan, Department of Anatomy and Medical Physiology, Division of Respiratory Medicine, Faculty of Medicine, University of Calgary, 293 H.M.R.B. 3330 Hospital Drive, N.W., Calgary, Alberta T2N 4N1, Canada, and Department of Biological Chemistry, Weizmann Institute of Science, 76100 Rehovot, Israel

Received March 30, 1999; Revised Manuscript Received July 6, 1999

ABSTRACT: ω-Conotoxin TxVII is the first conotoxin reported to block L-type currents. In contrast to other ω-conotoxins, its sequence is characterized by net negative charge and high hydrophobicity, although it retains the ω-conotoxin cysteine framework. In order to obtain structural information and to supply material for further characterization of its biological function, we synthesized TxVII and determined its disulfide bond pairings. Because a linear precursor with free SH groups showed a strong tendency to aggregate and to polymerize, we examined many different conditions for air oxidation and concluded that a mixture of cationic buffer and hydrophobic solvent was the most effective for the folding of TxVII. Synthetic TxVII was shown to suppress the slowly inactivating voltage-dependent calcium current in cultured *Lymnaea* RPeD1 neurons and furthermore to suppress synaptic transmission between these neurons and their follower cells. In contrast, TxVII did not block calcium flux through L-type channels in PC12 cells, suggesting a phyletic or subtype specificity in this channel family. Disulfide bond pairings of TxVII and its isomers were determined by enzymatic fragmentation in combination with chemical synthesis, thus revealing that TxVII has the same disulfide bond pattern as other ω-conotoxins. Furthermore, the CD spectrum of TxVII is similar to those of ω-conotoxins MVIIA and MVIIC. The precursor sequence of TxVII was determined by cDNA cloning and shown to be closest to that of δ-conotoxin TxVIA, a sodium channel inactivation inhibitor. Thus TxVII conserves the structural fold of other ω-conotoxins, and the TxVIA/TxVII branch of this family reveals the versatility of its structural scaffold, allowing evolution of structurally related peptides to target different channels.

Voltage-gated calcium channels play crucial roles in regulating intracellular calcium concentrations in a wide variety of cells and are classified into several subtypes according to their electrophysiological and pharmacological properties (*1*−*3*). Various specific peptide ligands have been used for pharmacological distinction of calcium channel subtypes, including the ω-conotoxins isolated from the venom of marine *Conus* snails. Thus the definitive ligands for N-type calcium channels are ω-conotoxins GVIA and MVIIA, while P/Q-type channels are blocked by ω-conotoxin MVIIC (*4*). In contrast, the only known peptide blockers of L-type calcium channels, calciseptine (*5*), and ω-agatoxin IIIA (*6*), are of limited efficacy and specificity. Therefore the most widely used pharmacological tools for L-type channels are dihydropyridine derivatives (*7*, *8*).

ω-Conotoxin TxVII was recently described from the venom of the molluscivorous snail *Conus textile* (*9*). This toxin blocks dihydropyridine-sensitive calcium channels in caudodorsal cell neurons from the mollusc *Lymnaea stagnalis* (*10*) and is so far the only conotoxin suggested to target L-type calcium channels. Despite being the first conotoxin blocker for L-type channels, the biological functions of TxVII[1] are not well elucidated due to a limited amount of native toxin. In contrast to other ω-conotoxins such as GVIA, MVIIA, and MVIIC, which are basic and hydrophilic peptides, TxVII is an acidic and hydrophobic peptide, although it retains the common ω-conotoxin cysteine framework (Figure 1). Interestingly, the sequence of TxVII resembles that of δ-conotoxin TxVIA, a sodium channel inactivation inhibitor (*11*).

† This work was supported in part by a project grant from the Japan Health Science Foundation, Program for Promotion of Fundamental Studies in Health Sciences of Organization for Drug ADR Relief, R&D Promotion and Product Review of Japan, an Israel−Japan Biotechnology collaborative grant (Israeli Ministry of Science), and the Dr. Josef Cohn Minerva Center for Biomembrane Research (Weizmann Institute).

* To whom correspondence should be addressed: Fax (81)42-724-6317; E-mail kazuki@libra.ls.m-kagaku.co.jp.

‡ Mitsubishi Kasei Institute of Life Sciences.

§ University of Calgary.

|| Weizmann Institute.

[1] Abbreviations: Acm, acetamidomethyl; DM, L-15 defined medium; Fmoc, 9-fluorenylmethoxycalbonyl; GSH, reduced glutathione; GSSG, oxidized glutathione; GVIA, ω-conotoxin GVIA; HEPES, *N*-(2-hydroxyethyl)piperazine-*N*′-ethanesulfonic acid; HPLC, high-performance liquid chromatography; HVA, high-voltage activated; MALDI-TOF-MS, matrix-assisted laser desorption/ionization time-of-flight mass spectrometry; MVIIA, ω-conotoxin MVIIA; MVIIC, ω-conotoxin MVIIC; RP-HPLC, reversed-phase high-performance liquid chromatography; Npys-Cl, 3-nitro-2-pyridinesulfenyl chloride; TFA, trifluoroacetic acid; Trt, trityl; TxVII, ω-conotoxin TxVII; TxVIA, δ-conotoxin TxVIA.

10.1021/bi990731f CCC: $18.00
Published on Web 09/03/1999

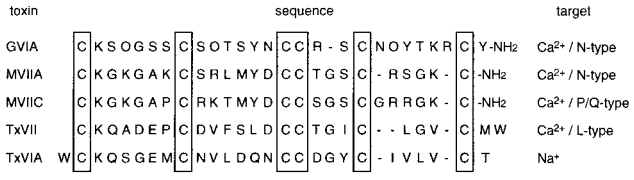

FIGURE 1: Amino acid sequences of TxVII and related conotoxins. The letters O and NH_2 represent *trans*-4-hydroxyproline and amidated carboxyl termini, respectively. The conserved cysteine framework is enclosed in rectangles. Disulfide bond pairings are previously determined for GVIA, MVIIA, and MVIIC, i.e., between the 1st and 4th, 2nd and 5th, and 3rd and 6th cysteines.

In the present study, we chemically synthesized TxVII and determined its disulfide bond pairings in order to obtain structural information as a base for structure−activity relationship studies and to prepare material for analysis of the biological functions of TxVII. Synthetic TxVII was shown to suppress the slowly inactivating/sustained calcium currents and, more interestingly, to suppress the synaptic transmission in cultured *Lymnaea* RPeD1 neurons. The precursor sequence of TxVII was determined by cDNA cloning and shown to be closest to that of δ-conotoxin TxVIA, a sodium channel inactivation inhibitor.

EXPERIMENTAL PROCEDURES

Materials. Fmoc-amino acids, Fmoc-Trp(Boc)-resin, and other reagents used on a synthesizer were obtained from Perkin Elmer−Applied Biosystems (Chiba, Japan). H-Cys-(Trt)-Trt(2-Cl)-resin and Fmoc-Gly-resin were obtained from Watanabe Chemicals Ltd. (Hiroshima, Japan). Npys-Cl was purchased from Kokusan Chemicals Ltd. (Tokyo, Japan). Lysyl endopeptidase and thermolysin were purchased from Wako Pure Chemicals Ltd. (Osaka, Japan).

Synthesis and Purification of Peptide. Solid-phase peptide synthesis was conducted on a Perkin Elmer−Applied Biosystems 433A peptide synthesizer. Amino acid analyses were performed on a Beckman System Gold amino acid analyzer after hydrolysis in 6 M hydrochloric acid at 110 °C for 24 h and derivatization by 4-(dimethylamino)azobenzene-4′-sulfonyl chloride. MALDI-TOF-MS was measured on a PerSeptive Biosystems Voyager Linear DE mass spectrometer, with α-cyano-4-hydroxycinnamic acid as a matrix. Analytical RP-HPLC was conducted on a Shimadzu LC-6A system with an ODS column Shim-pack CLC-ODS (4.6 × 250 mm, Shimadzu), or a C4 column YMC-pack AP803 S-5 C4 (4.6 × 250 mm, YMC). Preparative RP-HPLC was performed on a Shimadzu LC-8A system with an ODS column Shim-pack PREP-ODS (H) (20 × 250 nm, Shimadzu).

The linear precursor of TxVII assembled by Fmoc solid-phase synthesis (*12*) was cleaved from the resin with a mixture of TFA, H_2O, ethanedithiol, phenol, and thioanisole (percentage volume ratios 82.5/5/2.5/7.5/5). After being stirred for 2 h at room temperature, the solution was cooled and mixed with a 10-fold volume of *tert*-butyl methyl ether precooled at −20 °C. The resultant precipitates were collected on a glass filter and washed thoroughly with *tert*-butyl methyl ether. The deprotected peptide was extracted from the resin with 50% acetonitrile containing 0.1% TFA. After filtration, the peptide solution was added into 1.0 M ammonium acetate buffer (pH 7.8) or 0.4 M Tris-HCl buffer (pH 8.2), each containing EDTA (final 1 mM) and reduced and oxidized glutathione (final 5 and 0.5 mM, respectively). An organic solvent or a denaturing agent was added in some conditions. The resultant solutions contained the peptide at a calculated concentration of 0.05 mM. Some of the typical conditions and relative yields are listed in Table 1. Folding was allowed to proceed at 4 °C and monitored by analytical RP-HPLC. When close to equilibrium, the reaction was stopped by lowering the pH to 3−4 with acetic acid or 2 M HCl. TFA was then added to the solution to a final concentration of 0.1%. The acidified solution was further diluted with aqueous 0.1% TFA if the organic solvent or denaturing agent concentrations were high, filtered through both paper and 0.22 μm membrane filters, and then loaded onto an ODS column (30 × 250 mm) by a medium pressure pump. After nonadsorbed components had been washed out, the peptide was eluted with 50% acetonitrile containing 0.1% TFA. The crude peptide mix was subsequently purified by chromatography over Sephadex G-50F and preparative RP-HPLC with an ODS column. Identity of the synthetic peptide with native TxVII was verified by coinjection on an analytical RP-HPLC under four different conditions; (i) linear gradient of 5−75% acetonitrile in 0.1% TFA for 35 min on an ODS column, (ii) isocratic condition of 42% acetonitrile in 0.1% TFA on an ODS column, (iii) linear gradient of 5−75% acetonitrile in 0.1% TFA for 35 min on a C4 column, (iv) isocratic condition of 29% acetonitrile in 0.1% TFA on a C4 column. All RP-HPLC runs were performed at a flow rate of 1 mL/min. The structure and purity of the synthetic peptide was further confirmed by MALDI-TOF-MS measurement and amino acid analysis.

Table 1: Oxidative Disulfide Bond Formation of TxVII[a]

condition number	buffer[b]	MeCN (%)	MeOH (%)	detergent (M)	GSSG (mM)	GSH (mM)	relative yield[c]
1	A	5	0		0.5	5	1
2	A	5	0	guanidine 6.0	0.5	5	2
3	A	5	0	urea 8.0	0.5	5	8
4	A	35	0		0.5	5	10
5	A	5	20		0.5	5	1
6	A	5	50		0.5	5	14
7	B	5	0		0.5	5	2
8	B	5	0	guanidine 6.0	0.5	5	4
9	B	5	0	urea 8.0	0.5	5	9
10	B	35	0		0.5	5	150
11	B	5	20		0.5	5	48
12	B	5	50		0.5	5	260
13	B	5	50		0	10	7
14	B	5	50		1	0	216
15	B	5	50		0	0	22

[a] Linear TxVII extracted from resin with 50% MeCN/0.1% TFA was added at a final peptide concentration of 0.05 mM. All the tabulated values represent the final concentration of each component in the solutions, all of which contained 1 mM EDTA. The solutions were stirred at 4 °C until folding reaction reached equilibrium. [b] Buffer A, 1.0 M NH_4OAc (pH 7.8); buffer B, 0.4 M Tris-HCl (pH 8.2). [c] Estimated from peak area on analytical HPLC.

Determination of Disulfide Bond Combination. Synthetic peptide (0.2 mg) was incubated with 0.1 mg of lysyl endopeptidase in 420 μL of 0.5 M ammonium acetate buffer (pH 6.3) for 2 days at 37 °C. Digest products were purified over RP-HPLC separation and identified by MALDI-TOF-MS measurements. The major fragment thus obtained was lyophilized and further digested with thermolysin (20 μg) in 0.5 mL of 0.1 M ammonium formate buffer (pH 6.5) and 0.5 mM $CaCl_2$. The mixture was incubated at 37 °C for 16

h and the resultant peptide fragments containing disulfide bonds were separated on RP-HPLC and identified by MALDI-TOF-MS measurements. Elution profiles of authentic fragment A and those derived from synthetic TxVII and its isomer were compared by coinjection or individual injection on to an ODS column under isocratic conditions of 10% acetonitrile in 0.1% TFA at a flow rate of 1 mL/min.

An authentic peptide containing two disulfide bridges was synthesized by the method previously reported by Chino et al. (*13*) with some modifications. An octapeptide possessing two free thiol groups and one Acm-protected thiol group was synthesized by Fmoc chemistry and cyclized between free thiols by air oxidation in 0.2 M ammonium acetate buffer (pH 8.0) at a concentration of 0.15 mM. The solution was stirred at room temperature for 5 h, and then acidified with acetic acid and lyophilized. The peptide was dissolved in acetic acid containing equimolar Npys-Cl, and after stirring for 1 h, to the resulting solution was added acetic acid containing equimolar valylcysteine. After being stirred at room temperature for 2 h, the brown solution was diluted with water and separated with an equal volume of diethyl ether three times. The aqueous solution was lyophilized, and the bicyclic peptide was purified by preparative HPLC. The purified peptide (1 mg) and lysyl endopeptidase (0.1 mg) were incubated in 200 μL of 0.25 M ammonium acetate buffer (pH 6.3) at 37 °C for 16 h, and the product was subjected to HPLC separation and MALDI-TOF-MS measurements.

CD Measurement. CD spectra were recorded on a Jasco J-600 spectropolarimeter in H_2O solution (10 mM sodium phosphate, pH 7.0) at 20 °C, with a quartz cell of 1 mm path length. The spectra are expressed as molar ellipticity [θ].

Electrophysiology. Laboratory-raised stocks of the freshwater pond snail *Lymnaea stagnalis* were maintained in well-aerated artificial pond water (18−20 °C) and fed lettuce. Snails with a shell length of 15−20 mm (approximately 3−6 months old) were used in all experiments.

Animals were dissected under sterile conditions as described previously (*14*). Briefly, the central ring ganglia were isolated aseptically and treated with trypsin (Type III, 3 mg/mL, Sigma) for 25 min, followed by trypsin inhibitor (3 mg/mL, Sigma) for 10 min. The ganglia were pinned down to the bottom of a dissection dish and the identified respiratory interneuron, right petal dorsal 1 (RPeD1), was extracted from the intact ganglion by applying gentle suction via a fire-polished pipette (2 mm, WPI, lB200F). The isolated somata were plated on a poly(L-lysine)- (Sigma) coated dishes (Falcon 3001) containing L-15 defined medium (DM). The DM was composed of 50% (v/v) Liebowitz L-15 medium (Gibco), with additional salts (at the following millimolar concentrations: NaCl 40.0, KCl 1.7, $CaCl_2$ 4.1, $MgCl_2$ 1.5, and HEPES 5.0), 10 mM glucose, 1.0 mM L-glutamine, and 20 mg/mL gentamycin. The pH was adjusted to 7.9 with 1 M NaOH. All experiments were performed on cells that were maintained in DM for 12−24 h.

Whole-cell voltage-clamp (membrane ruptured) recordings were obtained by using Axopatch 1D amplifier (Axon Instruments, Foster, CA) in the single-electrode voltage-clamp mode. Patch electrodes (1−2 MW) were pulled in two steps on a vertical pipette puller (Kopf model 750, Tujunga, CA) from patch glass capillary tubing (PG150T-7.5, Warner Instrument Corp., Hamden, CT). Pipettes were filled with filtered (0.22 μm filter) pipette solution consisting of CsCl (29 mM), $CaCl_2$ (2.3 mM), ethylene glycol bis(2-aminoethyl ether)-*N*,*N*,*N*′,*N*′-tetraacetic acid (EGTA, 11 mM), HEPES (10 mM), ATP-Mg (2 mM), and GTP-Tris (0.1 mM), with pH 7.4 (adjusted with CsOH). The bath reference electrode was filled with bath solution, consisting of tetraethylammonium chloride (TEA-Cl, 47.5 mM), $MgCl_2$ (1 mM), $CaCl_2$ (4 mM), HEPES (10 mM), and 4-aminopyridine (4-AP, 2 mM), pH 7.9 (adjusted with TEA-OH). After GΩ seals were obtained, the series resistance was compensated by using membrane test function (pClamp-7, Axon Instruments). Following compensation, the series resistance was generally found to be less than 0.8 M. The Ca^{2+} current measured in this study was filtered at 1 kHz by use of a 4-pole Bessel filter and digitized at a sampling frequency of 5 kHz. The voltage command generation and data acquisition were carried out on a Dell (XPS R350) computer equipped with a Digidata 1200 interface (Axon Instruments) in conjunction with pClamp-7 software (Axon Instruments). The data were presented as the mean ± SD format. Differences between mean values from each experimental group were tested by Student's *t*-test and these were considered significant if $p < 0.05$.

Calcium Flux Measurements. PC12 cells were washed and suspended at 5×10^6 cells/mL in Locke's buffer (in millimolar concentrations: NaCl 154, KCl 5.6, $MgSO_4$ 1.2, $CaCl_2$ 2.2, glucose 10, and HEPES 5.0; pH 7.4). Loading with fluorescent dye was carried out for 45 min at 37 °C, with 5 μM Fluo4 (Molecular Probes) and 0.02% Pluronic F-127 (Sigma). After wash, cells were dispensed in 50 μL aliquots (250 000 cells), supplemented with toxins as required, and incubated for 15 min at room temperature. The cells were then depolarized by adding 150 μL of buffer containing 91 mM KCl (final $[K^+] = 70$ mM). Calcium influx was quantified on a Spectramax Gemini fluorescent plate reader (Molecular Devices Inc.) at an excitation wavelength of 494 nm, monitoring emission at 516 nm. All assays were performed in triplicate.

Cloning of TxVII Precursor Sequence. Venom duct cDNA from eight specimens of *Conus textile neovicarius* from the Northern Red Sea was used to construct a plasmid library. The library was cloned in the *Sma*I site of pBluescript, and 130 000 primary clones were obtained. A two-step PCR protocol was used to rapidly clone TxVII-encoding cDNAs, using library DNA as template. A degenerate antisense primer TxVII (5′ CAD ATN CCN GTR CAR CAR TC 3′) encompassing residues 14−20 of the mature TxVII peptide sequence was used in PCR versus T3 and T7 primers with Vent DNA polymerase. A 380-bp product was obtained when PCR was carried out with TxVII versus T3 primers. The product was cloned, and multiple clones were sequenced on both strands. All sequences were identical, and encoded a 70 amino acid open reading frame ending at the C-terminal on residues 1−20 of the mature TxVII sequence. To complete the whole precursor cDNA sequence, a specific sense primer (5′ AGG GGT ACC GCC ACC ATG AAA CTG ACG TGC ATG ATG ATC G) targeted at the start codon of the TxVII precursor was used against the T7 primer to obtain PCR products from the cDNA library. A single PCR product was isolated and cloned. Sequencing of multiple

clones revealed the entire TxVII cDNA sequence. Sequence alignments were made with CLUSTALX version 1.63b (*15*). Additional local alignments along the conserved cysteine residues were performed manually. The regions of the signal sequences were assigned by use of SignalP version 1.1 (*16*). A phylogenetic tree was generated with CLUSTALX from the aligned sequences and bootstrapped by the neighbor-joining method with 1000 iterations of bootstrap samplings to obtain confidence values (*17*). The nonrooted cladogram was displayed with TreeView (*18*).

RESULTS

Synthesis and Purification of TxVII. The linear precursor of TxVII from which all the protective groups had been removed was extracted from the resin with 50% aqueous acetonitrile containing 0.1% TFA and added directly into a folding solution without purification. Formation of correctly folded TxVII was monitored by comparison with native (venom-purified) TxVII on RP-HPLC. To obtain an optimum yield for the folding of TxVII, we have examined more than 100 conditions for air oxidation. Some of the typical conditions and relative yields are listed in Table 1. Ammonium acetate buffer (1 M, pH 7.8) containing GSSG and GSH (condition 1), which is used for efficient synthesis of MVIIA (*19*) and MVIIC (*20*), afforded only a minute amount of correctly folded TxVII. A large amount of precipitate formed during air oxidation. This is probably due to aggregation and polymerization of the peptide, since most of the crude cyclized products eluted earlier than the monomeric fraction upon gel-filtration chromatography. Addition of detergent improved the yields (conditions 2 and 3). TxVII is rich in hydrophobic residues and its folded isomers become even more hydrophobic than the linear form, as judged from retention times on RP-HPLC. We therefore tested solutions of increasing hydrophobicity containing organic solvents (conditions 4−6). Some of these conditions increased the efficiency of TxVII folding, with the best yield at 50% methanol as cosolvent (condition 6). Significant improvement was also observed when the buffer was changed from ammonium acetate (pH 7.8) to Tris-HCl (pH 8.2) (conditions 7−12). We further examined the effect of GSSG and GSH and found that lack of GSH did not lower the yield of TxVII notably, whereas lack of GSSG reduced correct folding. Reaction temperature, which has been shown to be crucial for folding of MVIIA or MVIIC, did not prominently influence the yield in the range from −20 to 37 °C in 50% methanol solution. Although the folding reaction reached maximum faster at higher temperature, prolonged reaction at 37 °C resulted in a decrease of peak height in RP-HPLC analysis.

Preparative amounts of TxVII were ultimately synthesized according to condition 12 in Table 1, with a folding solution containing 50% methanol, 5% acetonitrile, 0.4 M Tris-HCl (final pH 8.2), 1 mM EDTA, 0.5 mM GSSG, 5 mM GSH, and 0.05 mM linear peptide. Figure 2A shows the RP-HPLC profile of the reaction mixture. Compounds from peaks a and b were purified until they migrated as a single peak on an analytical RP-HPLC. Both compounds showed the same molecular weight ($MH^+ = 2835.3$) by MALDI-TOF-MS analysis, which is in good agreement with the calculated value for TxVII ($MH^+ = 2835.3028$), indicating that they are disulfide bond isomers. Figure 2B,C shows the RP-HPLC profiles of purified synthetic TxVII (peak a in Figure 2A) and semipurified native TxVII. Peaks c and d in Figure 2C

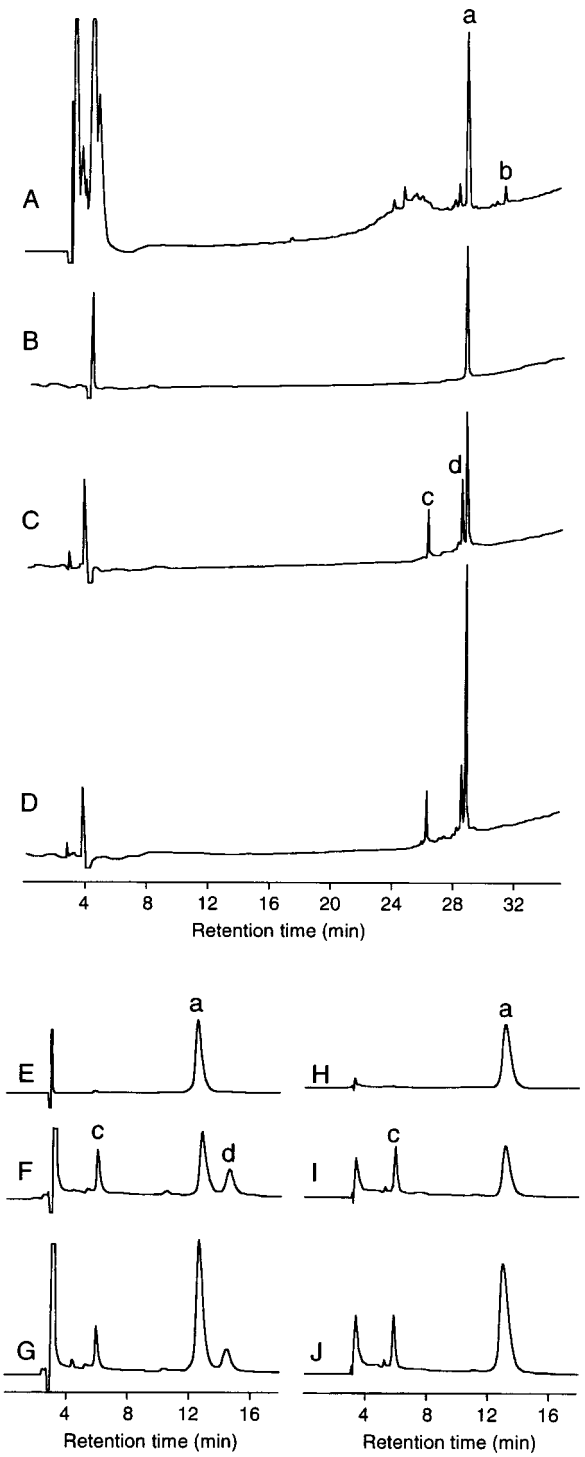

FIGURE 2: Reversed-phase HPLC profiles of (A) TxVII folding mixtures as obtained under condition 12 in Table 1; (B, E, H) purified synthetic TxVII; (C, F, I) native TxVII; and (D, G, J) coinjection of synthetic and native TxVII. Peak a, TxVII; peak b, TxVII isomer; peaks c and d, noncharacterized native peptides. In chromatograms A−D, peptides were eluted from an ODS column (4.6 × 250 mm) in a linear gradient of 5−75% acetonitrile with aqueous 0.1% TFA for 35 min at a flow rate of 1 mL/min. In chromatograms E−G, peptides were eluted from an ODS column (4.6 × 250 mm) in an isocratic condition of 42% acetonitrile in 0.1% aqueous TFA at a flow rate of 1 mL/min. In chromatograms H−J, peptides were eluted from a C4 column (4.6 × 250 mm) in an isocratic condition of 29% acetonitrile in 0.1% aqueous TFA at a flow rate of 1 mL/min.

yielded noncharacterized peptides with $MH^+ = 2850.9$ and 3113.6, respectively. Figure 2D shows a RP-HPLC profile of coinjected equal amounts of synthetic and native TxVII. Isocratic elution on RP-HPLC of synthetic and native TxVII also showed the same retention time in both coinjection and individual injection for both ODS (Figure 2E−G) and C4 (Figure 2H−J) columns, indicating that synthetic TxVII is identical to native toxin. The total synthesis from 0.25 mmol equivalent resin yielded 40 mg of TxVII and 1.6 mg of its isomer.

Determination of Disulfide Bond Pairing. We determined the disulfide bond pattern of synthetic TxVII and its isomer by the method previously described for the characterization of MVIIC isomers and MVIIC analogues (*21*, *22*). Successive digestion of synthetic TxVII and its isomer with lysyl endopeptidase and thermolysin gave a series of fragments, which were analyzed by RP-HPLC and MALDI-TOF-MS measurements. The most intense peak on the RP-HPLC corresponded to the C-terminal dipeptide (Met-Trp), and the other two intense peaks were derived from fragments containing the disulfide bond, designated as fragments A and B (Figure 3A). The identification of fragment B from the two peptides by RP-HPLC and MALDI-TOF-MS measurements revealed that both the peptides have a disulfide bond between Cys^8 and Cys^{20}. The two fragment A peptides also gave the same MH^+ value (1076.85 ± 0.2) irrespective of their different origin; however, their retention times on RP-HPLC were slightly different from each other.

There are two possible combinations of the four cysteines in fragment A, namely, Cys^1−Cys^{15}/Cys^{16}−Cys^{24} (broken line in Figure 3A) and Cys^1−Cys^{16}/Cys^{15}−Cys^{24} (solid line in Figure 3A). Each of these could correspond to the disulfide bond pairing of either synthetic TxVII or its isomer. To select the alternatives, we synthesized an authentic fragment A with disulfide bond pairing of Cys^1−Cys^{16}/Cys^{15}−Cys^{24} according to the scheme shown in Figure 3B. The two-step disulfide bond formation method gave a peptide containing a definite disulfide bond successfully in each step. Coinjection of the authentic fragment A and each fragment A derived from synthetic TxVII or its isomer clearly showed that the fragment A from synthetic TxVII was identical with the authentic fragment A, while that from the isomer was not (Figure 3C). Therefore, we concluded that TxVII has the same disulfide bond pairings as other ω-conotoxins, namely, Cys^1−Cys^{16}, Cys^8−Cys^{20}, and Cys^{15}−Cys^{24}. It follows that the disulfide bonding of the TxVII isomer is likely to be Cys^1−Cys^{15}, Cys^8−Cys^{20}, and Cys^{16}−Cys^{24}.

Secondary Structure Estimation from CD Spectra. In order to acquire further structural information, we measured the CD spectra of synthetic TxVII and its isomer (Figure 4). The spectrum of TxVII reveals two minima at around 205 and 280 nm and has overall features similar to those of MVIIA and MVIIC. The spectrum of the isomer is clearly different, with two maxima at around 210 and 285 nm, further supporting a structural difference between the two folding isomers of TxVII.

Synthetic TxVII Affected L-Type-like Ca^{2+} Currents in an Identified Respiratory Interneuron. To test whether synthetic TxVII blocks Ca^{2+} currents in the identified *Lymnaea* neuron right pedal dorsal 1 (RPeD1), the neuronal somata were isolated from the intact ganglia and maintained in cell culture. In DM, the isolated cells did not exhibit neurite outgrowth

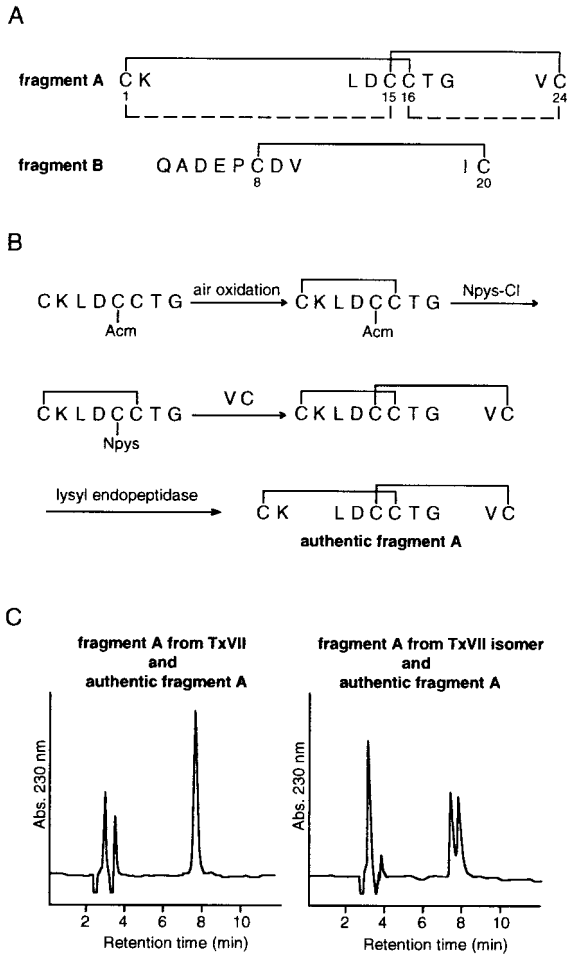

FIGURE 3: Determination of disulfide bond pairings of TxVII and its isomer. (A) Primary structures of fragments A and B, obtained from both TxVII and its isomer by successive digestion with lysyl endopeptidase (specific for C-terminus of a Lys residue) and thermolysin (specific for N-terminus of a hydrophobic amino acid residue). The solid line and the dashed line on the sequence of fragment A denote the alternative disulfide bond pairings. (B) Synthesis of authentic fragment A. The reaction condition in each step is described under Experimental Procedures. (C) Determination of identity between authentic fragment A and fragment A from synthetic TxVII or its isomer. All the peptides were injected as their molar equivalents were equal and eluted from an ODS column (4.6 × 250 mm) in an isocratic condition of 10% acetonitrile in 0.1% aqueous TFA at a flow rate of 1 mL/min.

and assumed a spherical shape within 12−24 h of culture (Figure 5). Whole-cell voltage-clamp recordings were made from the somata. Macroscopic Ca^{2+} currents were evoked by 450 ms depolarizing pulses applied from a holding potential of −80 to +35 mV, either in the absence or in the presence of synthetic TxVII. Figure 5 shows an example where bath-applied TxVII (20 μM) reduced the high-voltage-activated (HVA) Ca^{2+} current in RPeD1. The toxin-induced blockade of this Ca^{2+} current was reversible and occurred in the absence of any measurable shift in the $I-V$ relationship. Ca^{2+} current traces evoked by a voltage step from −80 to +5 mV (recorded from the same cell as shown in Figure 5) are presented in an inset. At depolarizing pulses applied from a holding potential of −80 to +5 mV, 20 μM synthetic TxVII reduced the peak L-type-like Ca^{2+} currents by 29% ± 14% ($n = 11$, $p < 0.05$). Since the dihydropyridine-blockable fraction of the current in these neurons is typically 35−40% of total calcium current (*36*), these effects of

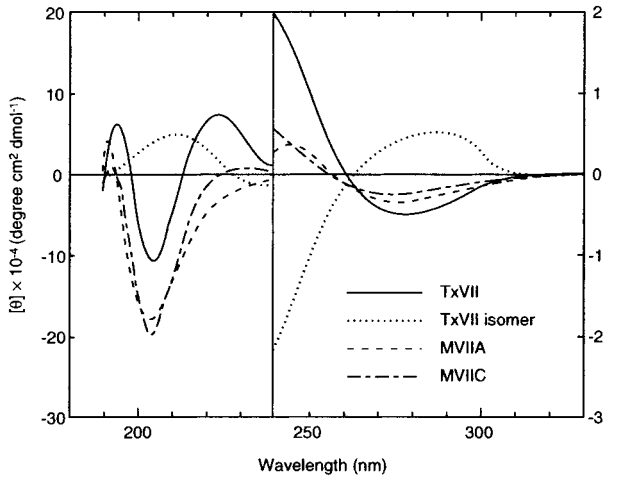

FIGURE 4: CD spectra of TxVII, its isomer, MVIIA, and MVIIC in H_2O solution (10 mM sodium phosphate, pH 7.0) at 20 °C. The spectra were recorded in the far-UV range (190−240 nm) and the near-UV range (240−330 nm) on a Jasco J-600 spectropolarimeter with a quartz cell of 1 mm path range. The vertical axis expresses molar ellipticity.

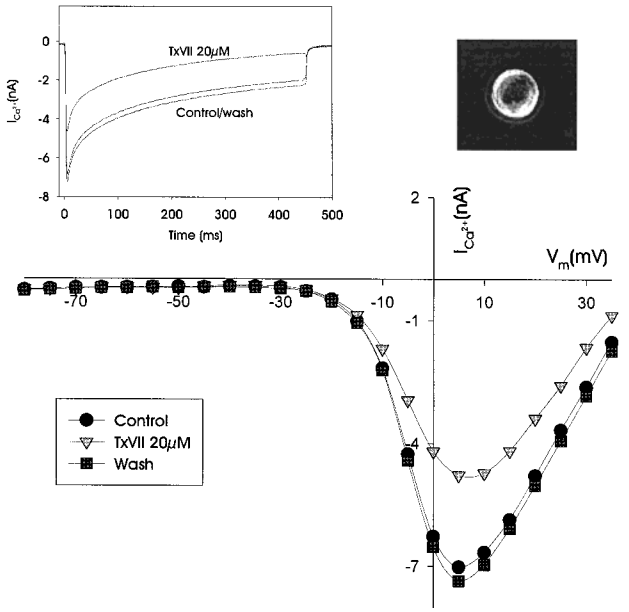

FIGURE 5: Synthetic TxVII blocked L-type like Ca^{2+} current in RPeD1. Whole-cell voltage clamp recordings were made from individually isolated somata of RPeD1. The $I-V$ relationship of Ca^{2+} current was obtained either in the absence (control and wash) or the presence of TxVII (20 μM) from cultured single RPeD1 (phase contrast photo; the diameter of the cell is 70 μm). Although bath-applied TxVII reduced the amplitude of the current in a voltage-dependent manner, it did not shift its current−voltage relationships. The inset shows Ca^{2+} current traces recorded at a voltage step from −80 mV to +5 mV in the absence (control/wash) or the presence of 20 μM TxVII. These data were collected from the same cell as shown in the figure.

synthetic TxVII reflect an almost complete block of the L-type-like current in RpeD1 cells. Furthermore, these effects were more pronounced when examined at the end of the depolarization pulse, where the current amplitude was reduced by 72% ± 15% (n = 11). This is consistent with the longer inactivation time of the sustained L-type current compared to the transient component that predominates in the early phase of the inward calcium current (*37*). Taken together, these data show that synthetic TxVII significantly and reversibly blocked the L-type-like Ca^{2+} current in cultured *Lymnaea* RPeD1 neurons, similar to the previously described effects of the native toxin on *Lymnaea* neurons (*9*).

In order to examine effects of synthetic TxVII on vertebrate L-type calcium channels, we carried out fluorescent measurements of voltage-driven calcium fluxes in PC12 cells. The cells were loaded with the calcium-sensitive dye Fluo4 as described under Experimental Procedures, and calcium influx was measured after depolarization with KCl. A voltage-induced calcium influx averaging 500 relative fluorescence units was obtained in this system. In the presence of the well-characterized L-type blocker nifedipine (10 μM), the flux was reduced to 45.7% ± 9.3% (mean ± SD, n = 3) of control levels, indicating that approximately half of the calcium current thus observed was through L-type channels. However, in the presence of 20 μM TxVII the observed calcium flux was 111.5% ± 13.2% (mean ± SD, n = 3) of control. Thus it appears that synthetic TxVII does not effectively block L-type calcium channels in PC12 cells.

Sequence and Phylogenetic Analysis of the TxVII Precursor cDNA. To characterize the cDNA sequence of the TxVII precursor, we cloned it by PCR. A degenerate antisense primer was constructed from the amino acid sequence data of mature TxVII (*9*) and used for PCR versus the T3 primer for pBluescript. The product thus obtained encodes a 70-amino acid open reading frame (ORF) containing at the C-terminal end the mature TxVII toxin sequence ending on the antisense cloning primer. A full-length cDNA sequence was obtained by using a sense primer on the start codon of the ORF versus a T7 primer for PCR on the cDNA library. A single PCR fragment was obtained and multiple subclones were sequenced. The predicted length of the TxVII precursor is 77 amino acids, which falls in the 73−82-amino acid range of other precursors of conotoxins based on their sequenced cDNAs (Figure 6A). Multiple sequence alignments were performed for the TxVII precursor sequence against five conotoxin cDNA sequences found in GenBank, as follows: TxVI-Ph from the Philippines form of *C. textile* [formerly designated as King-Kong 0 (*23*) or TxVIA (*24*)]; KK-1 and KK-2 from *C. textile* (*23*); MrVIB from *Conus marmoreus* (*25*); and GVIA from *Conus geographus* (*26*). An additional sequence for the Red Sea variant of TxVIA (TxVIA-RS) from *C. textile neovicarius* was obtained from an EST sequencing program on our *C. textile* library (S. Conticello and M. Fainzilber, unpublished results). The precursor amino acid sequence alignment with assigned signal, propeptide, and mature sequences as well as the well-conserved six cysteine-four loop residues is shown in Figure 6B. To visualize evolutionary relationships between precursor conotoxin sequences, an inferred nonrooted phylogenetic tree was constructed on the basis of the sequence alignments by the neighbor-joining method (*17*) (Figure 6C).

DISCUSSION

The hydrophobicity and acidity of TxVII distinguishes it from the hydrophilic and basic nature of most other ω-conotoxins (*9*). Consequently, folding conditions optimized for syntheses of ω-conotoxins MVIIA (*13*) or MVIIC (*14*) proved unsuitable for TxVII and resulted in formation of large amounts of precipitate. The results of the present study

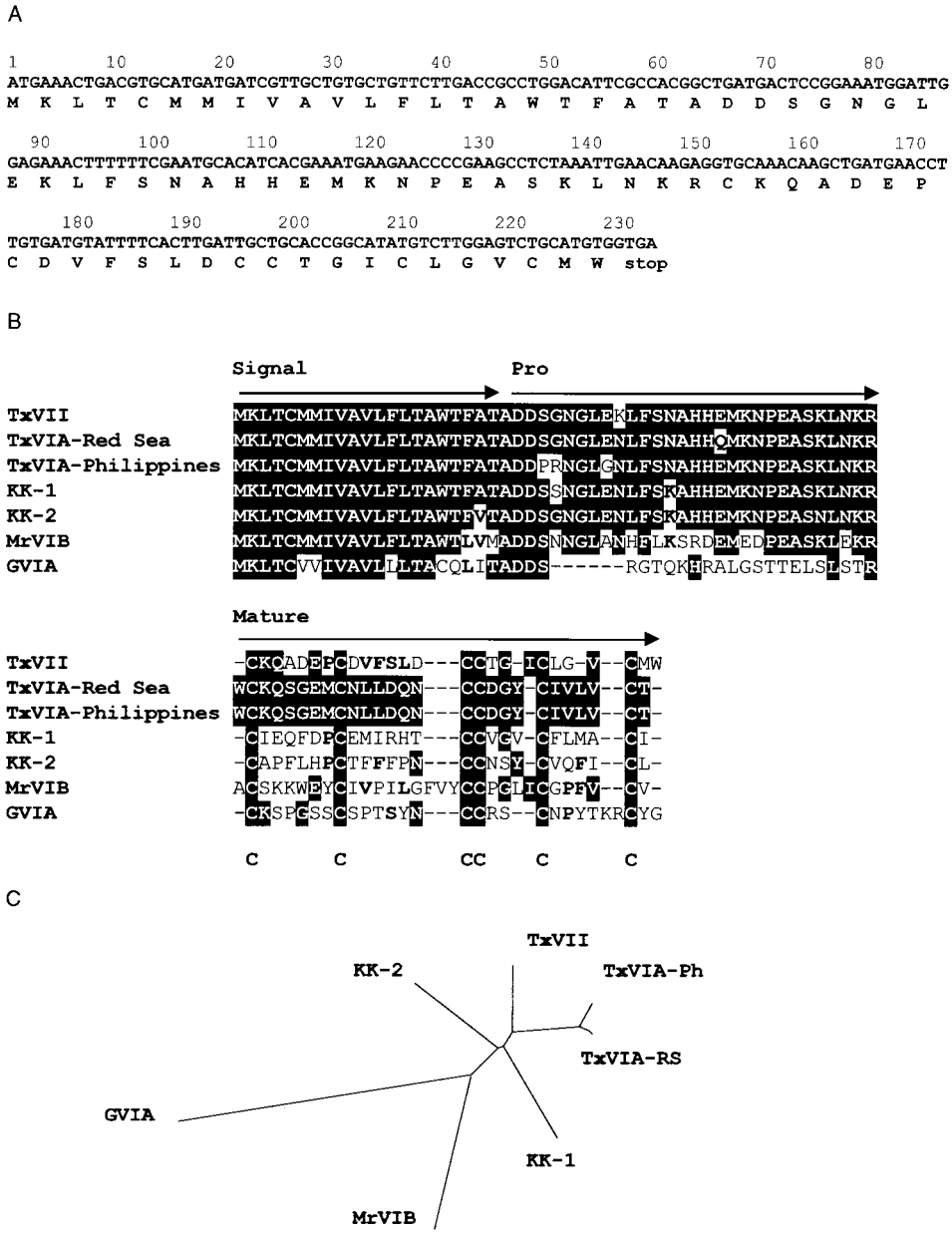

FIGURE 6: (A) cDNA sequence and predicted amino acid sequence of the TxVII toxin precursor. (B) Multiple sequence alignment of the precursor conotoxin sequence of TxVII versus other conotoxin precursors. TxVIA-Red Sea, TxVIA-Philippines [117742] (*24*), KK-1 [117743], and KK-2 [117744] (*23*) are from *C. textile*, while MrVIB [S78990] (*25*) is from *C. marmoreus*, and GVIA [461869] (*26*) is from *C. geographus*. Significant homologies are shown blocked while minor homologous amino acids are shown in boldface type. The signal, propeptide, and mature regions are indicated above the sequences with arrows. The conserved cysteine framework is indicated below the sequences. (C) Nonrooted phylogenetic tree of TxVII precursor with other conotoxin precursors. Branch lengths (values not indicated) are additive and indicative of the relative degree of homology between the precursor amino acid sequences.

are consistent with a model whereby linear synthetic TxVII tends to aggregate in a hydrophilic environment, followed by forming of intermolecular disulfide bonds. The positive effect of organic solvents or detergent on folding of TxVII would thus be explained in terms of an isolating effect, which favors intramolecular disulfide bond formation. Examination of salt effects on folding further accentuates the different requirements of the TxVII sequence. Whereas anion effects were previously shown to be crucial for folding of the highly basic conotoxin MVIIC (*21*), our current study clearly shows that Tris-HCl is more efficient than ammonium acetate for folding of TxVII. The predominance of acidic residues in TxVII suggests that the protonated tris(hydroxymethyl) amine ion is a better countercation for anions in the peptide, although part of the Tris effect might also be attributed to its relative hydrophobicity. This suggests that intramolecular repulsion between acidic residues might be the predominant electrostatic force obstructing correct folding of TxVII. The methods established in this study for efficient preparation of TxVII are likely to be applicable to other hydrophobic peptides that tend to aggregate during folding. Thus efficient in vitro folding of small cysteine-rich hydrophobic sequences will be favored by the combination of an isolating organic solvent with appropriate counterions for the predominant charged residues in the peptide.

The inefficient in vitro folding of TxVII raises speculations concerning facilitatory in vivo mechanisms for biosynthesis and folding of this and similar sequences. These might include disulfide isomerases, molecular chaperones, or other factors. Indeed, Woodward et al. (*27*) have previously

suggested that the propeptide domain in conotoxins might provide an intramolecular chaperone to facilitate folding of the mature peptide. However, subsequent in vitro studies of Price-Carter et al. (*28, 29*) suggested that the precursor sequence does not play a crucial role in the folding of MVIIA. A caveat for those studies is the hydrophilic nature of MVIIA, which allows relatively facile folding in solution, in contrast to the results of the present study on TxVII. Therefore, the possibility that the propeptide domain plays a role in folding is still open, and indeed hydrophobic sequences recalcitrant to folding such as TxVII are likely to prove most informative for such studies in the future.

Fragmentation of TxVII with endopeptidases and synthesis of an authentic fragment clearly showed that TxVII has the same disulfide bonding pattern as other ω-conotoxins, i.e., $Cys^{1}-Cys^{16}$, $Cys^{8}-Cys^{20}$, and $Cys^{15}-Cys^{24}$. Structural analysis of TxVII was further supplemented by comparative CD spectra, revealing that the CD spectrum of TxVII is similar to those of MVIIA and MVIIC. The disulfide isomer of TxVII exhibits a different CD spectrum, indicating a different structure imposed by the nonnative disulfide pairing. The classical ω-conotoxin GVIA contains three tyrosines, which affect its CD spectrum; however a $Tyr^{27} \rightarrow$ Ala GVIA mutant also exhibits a CD spectrum similar to that of TxVII [this mutation does not affect GVIA activity (*30*)]. Thus, as long as aromatic chromophores do not affect the spectra, ω-conotoxins ranging from the hydrophilic and highly basic GVIA to the hydrophobic and acidic TxVII exhibit similar CD spectra.

The three-dimensional solution structures of GVIA, MVIIA, and MVIIC have been determined by two-dimensional NMR, revealing a triple-stranded antiparallel β-sheet as their common structural motif (*31*−*34*). Taken together, the disulfide pairing and CD spectra determined in the current study suggest that TxVII shares this basic structural fold of ω-conotoxins. Previously, we have shown that Tyr^{13} is a common active site of GVIA (*35*), MVIIA (*19*), and MVIIC (*20*) and that the amino acid residues restricted to the N-terminal half are important for the recognition of N-type channels, whereas essential residues for P/Q-type channel recognition are widely spread over the whole ω-conotoxin molecule (*22*). If TxVII has a similar structural motif to those of other ω-conotoxins, it will be of much interest to determine the amino acid residues in TxVII essential for the its calcium channel subtype selectivity. In order to address these issues, synthesis of Ala-scanning analogues of TxVII and the analysis of three-dimensional structure by NMR are currently in progress.

Purified native TxVII effects on Ca^{2+} currents were originally tested only on caudodorsal cells of *Lymnaea* (*9*), due to limited amounts of venom-purified toxin. That study found that the L-type-like Ca^{2+} currents in these neurons (*10*) were significantly and reversibly blocked by the purified toxin TxVII (*9*). In the present study we opted to use an identified neuron (RPeD1) whose intrinsic, synaptic, network, and functional properties are well-characterized at the level of a single cell. The slowly inactivating HVA Ca^{2+} currents recorded from RPeD1 cells exhibited the pharmacological and biophysical properties of the L-type Ca^{2+} channel previously observed in the CDC cells (*10*). Moreover, venom-purified native toxin also reversibly blocked the L-type Ca^{2+} currents in RPeD1 (data not shown). In the present study, synthetic TxVII was found to significantly and reversibly block the L-type Ca^{2+} current in RPeD1. Since the toxin did not alter the $I-V$ relationship of this current, it seems that TxVII binding to the Ca^{2+} channel does not affect the voltage-dependent properties of its channel proteins. These findings are consistent with earlier studies on the CDC cells where the purified toxin, although it blocked the L-type-like Ca currents, did not affect their $I-V$ relationship (*9*). It therefore appears that the functional properties of the synthesized toxin are similar to those of the purified peptide and that its effects on HVA Ca^{2+} currents are widespread in the *Lymnaea* central nervous system. However, TxVII did not block calcium flux through L-type channels in PC12 cells (which are of rat origin). This suggests that the L-type channel family may reveal either subtype or phyletic subdivisions, which should be distinguishable by use of TxVII and related toxins as pharmacological tools. Further analyses of TxVII effects on a wide range of preparations should shed light on this issue. In any case the selective and reversible effects of TxVII on molluscan neurons suggest that this toxin will be a useful tool for studies on the roles of calcium channels in synaptic mechanisms under study in these systems. Since TxVII selectively and reversibly blocked the HVA Ca^{2+} channels in RPeD1 cells, this toxin should prove a useful tool for studies on the role of Ca^{2+} channels in synaptic mechanisms by which respiratory rhythm is generated in the intact animals (*14, 36*).

Cloning of the full-length TxVII precursor cDNA sequence revealed that this 26 residue conotoxin is initially translated as a prepropeptide of 77 amino acids. The cDNA open reading frame encodes signal and propeptide regions with the mature toxin located at the C-terminal end, similar to the prepropeptide organization found in other conotoxins (*29*). Multiple sequence alignment of the TxVII prepropeptide against other known conotoxin precursor sequences revealed significant homology between the signal and propeptide region of the precursors and hypervariability in the mature region except the cysteines, as expected for conotoxin cDNAs. Phylogenetic analysis of the TxVII precursor based on a nonrooted phylogenetic tree reveals that its overall sequence is evolutionarily closest to that of TxVIA, further strengthening the argument that TxVIA and TxVII may be the result of a recent gene duplication and subsequent divergent selection to different targets.

The results in this study confirmed that, despite its divergent sequence, TxVII has the canonical structural fold of all other ω-conotoxins. In terms of homology of sequences, TxVII constitutes a subclass together with δ-conotoxin TxVIA, the structural information of which has not been obtained except for its sequence. TxVIA is likely therefore to form the same structural motif as the ω-conotoxins, which indicates that this structural scaffold can accommodate diverse sequences and differing biological activities. Synthetic approaches to artificial ion channel blocking peptides are focused on developing more potent toxins with higher selectivity as pharmacological tools. The ω-conotoxin scaffold has clearly served as a successful basis for evolutionary elaboration of many such tools. Future work should take up the challenge of further modifications on this theme, to invent peptides with yet more diverse and selective activities.

ACKNOWLEDGMENT

We thank Drs. Masami Takahashi and Toshiyuki Kohno at Mitsubishi Kasei Institute of Life Sciences for helpful discussion and Dr. Silvestro Conticello at the Weizmann Institute for the TxVIA EST sequence and generous advice.

REFERENCES

1. Tsien, R. W., Ellinor, P. T., and Horne, W. A. (1991) *Trends Pharmacol. Sci. 12*, 349−354.
2. Miller, R. J. (1992) *J. Biol. Chem. 267*, 1403−1406.
3. Randall, A., and Tsien, R. W. (1995) *J. Neurochem. 15*, 2995−3012.
4. Olivera, B. M., Miljanich, G. P., Ramachandran, J., and Adams, M. E. (1994) *Annu. Rev. Biochem. 63*, 823−867.
5. De Weille, J. R., Schweitz, H., Maes, P., Tartar, A., and Lazdunski, M. (1991) *Proc. Natl. Acad. Sci. U.S.A. 88*, 2437−2440.
6. Mintz, I. M., Venema, V. J., Adams, M. E., and Bean, B. P. (1991) *Proc. Natl. Acad. Sci. U.S.A. 88*, 6628−6631.
7. Catterall, W. A., and Striessnig, J. (1992) *Trends Pharmacol. Sci. 13*, 256−262.
8. Hofmann, F., Biel, M., and Flockerzi, V. (1994) *Annu. Rev. Neurosci. 17*, 399−418.
9. Fainzilber, M., Lodder, J. C., van der Schors, R. C., Li, K. W., Yu, Z., Burlingame, A. L., Geraerts, W. P. M., and Kits, K. S. (1996) *Biochemistry 35*, 8748−8752.
10. Dreijer, A. M. C., and Kits, K. S. (1995) *Neuroscience 64*, 787−800.
11. Fainzilber, M., Kofman, O., Zlotkin, E., and Gordon, D. (1994) *J. Biol. Chem. 269*, 2574−2580.
12. Fields, G. B., and Noble, R. L. (1990) *Int. J. Pept. Protein Res. 35*, 161−214.
13. Chino, N., Kubo, S., Nishiuchi, Y., Kumagaye, S., Kumagaye, Y., Takai, M., Kimura, T., and Sakakibara, S. (1988) *Biochem. Biophys. Res. Commun. 151*, 1285−1292.
14. Syed, N. I., and Winlow, W. (1991) *J. Comp. Physiol. 169*, 557−568.
15. Thompson, J. D., Higgins, D. G., and Gibson, T. J. (1994) *Nucleic Acids Res. 22*, 4673−4680.
16. Nielsen, H., Engelbrecht, J., Brunak, S., and von Heijne, G. (1997) *Protein Eng. 10*, 1−6.
17. Saito, N., and Nei, M. (1987) *Mol. Biol. Evol. 4*, 406−425.
18. Page, R. D. M. (1996) *Comput. Appl. Biosci. 12*, 357−358.
19. Kim, J.-I., Takahashi, M., Ohtake, A., Wakamiya, A., and Sato, K. (1995) *Biochem. Biophys. Res. Commun. 206*, 449−454.
20. Kim, J.-I., Takahashi, M., Martin-Moutot, N., Seager, M. J., Ohtake, A., and Sato, K. (1995) *Biochem. Biophys. Res. Commun. 214*, 305−309.
21. Kubo, S., Chino, N., Kimura, T., and Sakakibara, S. (1996) *Biopolymers 38*, 733−744.
22. Sato, K., Raymond, C., Martin-Moutot, N., Sasaki, T., Omori, A., Ohtake, A., Kim, J.-I., Kohno, T., Takahashi, M., and Seager, M. J. (1997) *FEBS Lett. 414*, 480−484.
23. Woodward, S. R., Cruz, L. J., Olivera, B. M., and Hillyard, D. R. (1990) EMBO J. *9*, 1015−1020.
24. Fainzilber, M., Kofman, O., Zlotkin, E., Gordon, D. (1994) *J. Biol. Chem. 269*, 2574−2580.
25. McIntosh, J. M., Hasson, A., Spira, M. E., Gray, W. R., Li, W., Marsh, M., Hillyard, D. R., and Olivera, B. M. (1995) *J. Biol. Chem. 270*, 16796−16802.
26. Olivera, B. M., McIntosh, J. M., Cruz, L. J., Luque, F. A., and Gray, W. R. (1984) *Biochemistry 23*, 5087−5090.
27. Woodward, S. R., Cruz, L. J., Olivera, B. M., and Hillyard, D. R. (1990) *EMBO J. 9*, 1015−1020.
28. Price-Carter, M., Gray, W. R., and Goldenberg, D. P. (1996) *Biochemistry 35*, 15537−15546.
29. Price-Carter, M., Gray, W. R., and Goldenberg, D. P. (1996) *Biochemistry 35*, 15547−15557.
30. Kim, J.-I., Ohtake, A., and Sato, K. (1997) *Biochem. Biophys. Res. Commun. 230*, 133−135.
31. Davis, J. H., Bradley, E. K., Miljarnich, G. P., Nadasdi, L., Ramachandran, J., and Basus, V. J. (1993) *Biochemistry 32*, 7396−7405.
32. Pallaghy, P. K., Duggan, B. M., Pennington, M. W., and Norton, R. S. (1993) *J. Mol. Biol. 234*, 405−420.
33. Kohno, T., Kim, J.-I., Kobayashi, K., Kodera, Y., Maeda, T., and Sato, K. (1995) *Biochemistry 34*, 10256−10265.
34. Farr-Jones, S., Miljanich, G. P., Nadasdi, L., Ramachandran, J., and Basus, V. J. (1995) *J. Mol. Biol. 248*, 106−124.
35. Kim, J.-I., Takahashi, M., Ogura, A., Kohno, T., Kudo, Y., and Sato, K. (1994) *J. Biol. Chem. 269*, 23876−23878.
36. Feng, Z.-P., Hamakawa, T., Takasaki, M., Lukowiak, K., and Syed, N. I. (1997) *Soc. Neurosci. Annu. Meet. 23*, 1047.
37. Kits, K. S., Lodder, J. C., van der Schors, R., Li, K. W., Geraerts, W. P. M., and Fainzilber, M. (1996) *J. Neurochem. 67*, 2155−2163.

BI990731F